



Gamma relaxation in Dy-based metallic glasses and its correlation with plasticity

Liliang Shao^a, Lin Xue^b, Jichao Qiao^c, Qing Wang^d, Qianqian Wang^{a,e}, Baolong Shen^{a,*}

^a School of Materials Science and Engineering, Jiangsu Key Laboratory of Advanced Metallic Materials, Southeast University, Nanjing 211189, China

^b College of Mechanics and Materials, Hohai University, Nanjing 211100, China

^c School of Mechanics, Civil Engineering and Architecture, Northwestern Polytechnical University, Xi'an 710072, China

^d Laboratory for Microstructures, Institute of Materials Science, Shanghai University, Shanghai 200072, China

^e School of Materials Science and Engineering, Jiangsu Key Laboratory of Advanced Structural Materials and Application Technology, Nanjing Institute of Technology, Nanjing 211167, China

ARTICLE INFO

Keywords:

Metallic glasses
Relaxation spectrum
Fast γ relaxation
Mechanical property
Loosely packed region

ABSTRACT

The discovery of secondary relaxation in metallic glass (MG) breaks the longstanding cognition that MG, as a simple glassy system, exhibits only α relaxation and contributes significantly to the understanding of the structure and mechanical properties of MG. In this work, two independent fast secondary relaxation peaks corresponding to γ and β' relaxation were detected by dynamic mechanical measurement in several Dy-based MGs at temperatures far below the glass transition temperature. Compared with β' relaxation, the novel γ relaxation is activated at lower temperatures and possesses smaller activation energy approximately 2/3 of that for β' relaxation. By exciting γ relaxation, loosely packed regions evolve into vein-like patterns in the fracture surface, leading to unusual plasticity at cryogenic temperatures. Furthermore, a holistic relaxation spectrum including boson peak, fast γ and β' relaxation, slow β relaxation and primary α relaxation in MG was depicted.

Glassy materials play an essential role in human society, such as polymeric glasses for biotechnology, oxide glasses for optics and electronics and metallic glasses (MGs) for magnetics [1–4]. Owing to the long-range disordered structure and metastable state, glass undergoes absorbing relaxation under thermal agitation, which has attracted broad interest from both scientific studies and engineering applications [5–8]. Structurally complicated glasses such as molecular glasses possessing a hierarchical structure composed of main molecular chains, chain branches and functional groups usually exhibit a complex relaxation spectrum, including α relaxation, β relaxation, even γ relaxation and so on and so forth [6]. By comparison, MGs were once deemed to have only a single α relaxation related to glass transition because of their simple structure the seemingly random packing of atoms, and the lack of rotational degrees of freedom [9].

With the development of experimental characterization and computer simulation, it has been found that there are abundant and complicated short-range and medium-range orders in MGs [10,11], i.e., MGs are intrinsically heterogeneous at atomic and nanoscale [7,12,13]. The activation of hierarchically local structure is supposed to result in different physical responses. From this point of view, MGs are also

potential glassy system with multiple relaxation modes, and extensive studies verify this [14]. MGs can also exhibit a secondary β relaxation manifesting as peak, shoulder or excess wing on the dynamic mechanical spectrum (DMS) [15]. As a precursor to α relaxation, the discovery of β relaxation has greatly promoted the research of MGs. This relaxation mode is correlated with many unresolved issues in glassy physics and material sciences, including shear transformation zone [16], atomic diffusion [17] and liquid fragility [18], and has a crucial influence on the mechanical, magnetic and chemical properties of MGs [19–21]. Recently, an additional relaxation peak emerging at a lower temperature than that of β relaxation has been detected in various MGs, i.e., fast β' relaxation [22,23]. The strength of β' relaxation is $\sim 1/10$ of β relaxation with the activation energy $\sim 1/2$ of β relaxation. Hence, β' relaxation can be regarded as a trigger process for β relaxation. It is noteworthy that a new relaxation process defined as γ relaxation was reported in Zr- and Pd-based MGs [24], the temperature range of which is approximately $0.2\text{--}0.3 T_g$ (glass transition temperature). This ultralow temperature relaxation is very akin to the long known γ relaxation in amorphous polymers [25,26]. However, only one low-temperature relaxation peak was detected on the DMS and it is similar to β' relaxation peaks observed

* Corresponding author,

E-mail address: blshen@seu.edu.cn (B. Shen).

<https://doi.org/10.1016/j.scriptamat.2022.115017>

Received 8 June 2022; Received in revised form 8 August 2022; Accepted 26 August 2022

1359-6462/© 2022 Acta Materialia Inc. Published by Elsevier Ltd. All rights reserved.

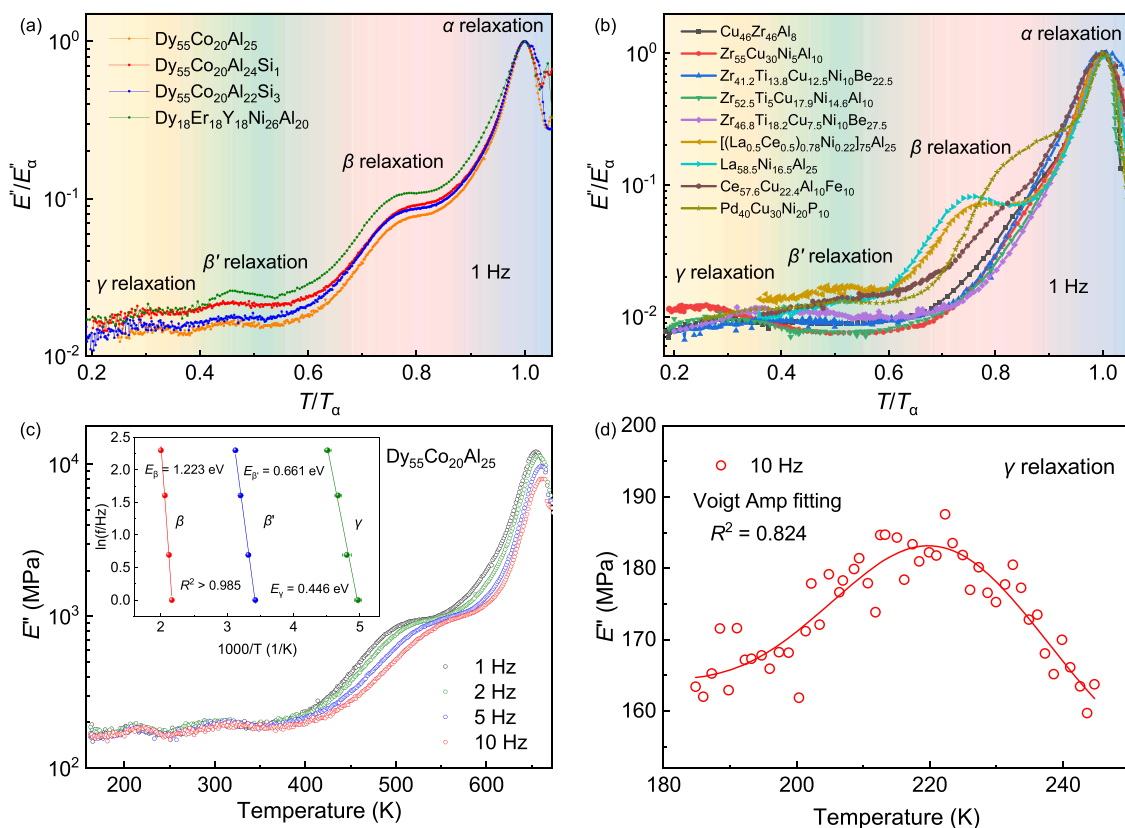


Fig. 1. (a) Temperature dependence of loss modulus (E'') curves for the four RE-based BMGs with novel γ relaxation under a frequency of 1 Hz and heating rate of 2 K/min. E'' is normalized by the corresponding maximum value at T_{α} and temperature is scaled by T_{α} . (b) Comparison of the temperature-dependent E'' curves of some typical MGs. The data were collected from Ref. [27]. (c) Temperature-dependent E'' with the driven frequency ranging from 1 to 10 Hz for the $Dy_{55}Co_{20}Al_{25}$ BMG. The inset shows the frequency dependence of T_{β} , $T_{\beta'}$ and T_{γ} fitted by Arrhenius relation. The goodness-of-fit (R^2) values for three secondary relaxations are larger than 0.985. (d) Magnification of the $E''(T)$ curve corresponding to γ relaxation.

in some other MGs [27]. Is the so-called γ relaxation a novel relaxation mode different from β' relaxation? In that event, are there any correlations between γ relaxation and mechanical property like other secondary relaxations of MGs? To elucidate these questions, more systematic investigations of the ultralow temperature relaxation of MGs are urgently needed.

In this work, compelling experimental evidence of two individual low-temperature peaks on DMS of several Dy-based MGs indicates that there is a novel fast relaxation different from β' relaxation, i.e., γ relaxation in MGs. The activation of γ relaxation leads to unusual plasticity at cryogenic temperatures. Moreover, a holistic relaxation spectrum of MG from the initial state boson peak to the final state crystallization was established.

Glass-forming alloy ingots were prepared by arc-melting or induction melting mixtures of pure metals under argon atmosphere according to the alloy feature. The purities of all raw metals are better than 99.9 wt. %. $Dy_{55}Co_{20}Al_{25-x}Si_x$ ($x = 0, 1, 3$) and $Dy_{18}Er_{18}Y_{18}Ni_{26}Al_{20}$ bulk metallic glasses (BMGs) samples were prepared by copper mold casting, and glassy ribbons were fabricated by single-roll melt spinning. The amorphous nature of the as-cast and as-quenched samples was confirmed by X-ray diffraction (XRD, Bruker D8 Discover) and differential scanning calorimetry (DSC, Netzsch 404 F3). The corresponding XRD patterns and DSC traces of the studied MGs are shown in Figs. S1 and S2, indicating the whole amorphous structures of the used samples. The relaxation behaviors of the selected rare earth (RE)-based BMGs were characterized by a dynamic mechanical analyzer (DMA, TA Q800). BMG samples with dimensions of 30 mm \times 2 mm \times 1 mm and single cantilever bending were used for DMA tests. For the Fe-based MGs, glassy ribbons with a thickness of 20–30 μ m and width of 1–1.5 mm as well as film tension mode were applied by a DMA (Netzsch 242E). BMG rods with a diameter

of 2 mm and height of 4 mm were used for compression tests. Uniaxial compression tests were carried out over a temperature range from 203 to 293 K with a constant strain rate of $5 \times 10^{-4} s^{-1}$. The fracture morphology of the BMG rods after compression was characterized by scanning electron microscopy (SEM, FEI Sirion 200). The nanoscale structural features of BMG samples were observed by high-resolution transmission electron microscopy (HRTEM, Talos F200X). The sample for TEM observation was prepared by ion milling method (Gatan INC PIPS-M691) under liquid nitrogen cooling condition.

Fig. 1(a) shows the temperature dependence of the loss modulus (E'') for $Dy_{55}Co_{20}Al_{25-x}Si_x$ ($x = 0, 1, 3$) and $Dy_{18}Er_{18}Y_{18}Ni_{26}Al_{20}$ BMGs. As expected, a sharp α relaxation around T_g coupled with a prominent β relaxation shoulder was detected for all of the BMG samples. It is striking that in addition to the above two common relaxation processes, two more weak and broad humps can be observed at temperature region of 0.2–0.6 T_{α} . According to previous reports [27], a fast relaxation mode, i. e., β' relaxation is activated in this temperature range. However, there are two independent humps in the studied BMGs. In order to distinguish the two processes, the hump at lower temperature is termed as γ relaxation. Compared with β' relaxation, the strength of γ relaxation is lower, $\sim 1/2$ – $2/3$ of β' relaxation. The peak temperature of γ relaxation is near 0.3 T_{α} , whereas β' relaxation takes place at higher temperatures next to β relaxation. Actually, γ relaxation is widespread in MGs, but it has not been distinguished from β' relaxation and no relaxation spectrum with two obvious humps at low temperatures was detected before. As shown in Fig. 1(b), we summarized the DMS of various MGs [27]. It is seen that several Zr- and CuZr-based MGs show remarkable humps at temperatures of 0.2–0.4 T_{α} , which is consistent with the γ relaxation observed in this study. It is noteworthy that two coupled humps develop successively on the DMS of some Fe-based MGs as shown in Figs. S7 and

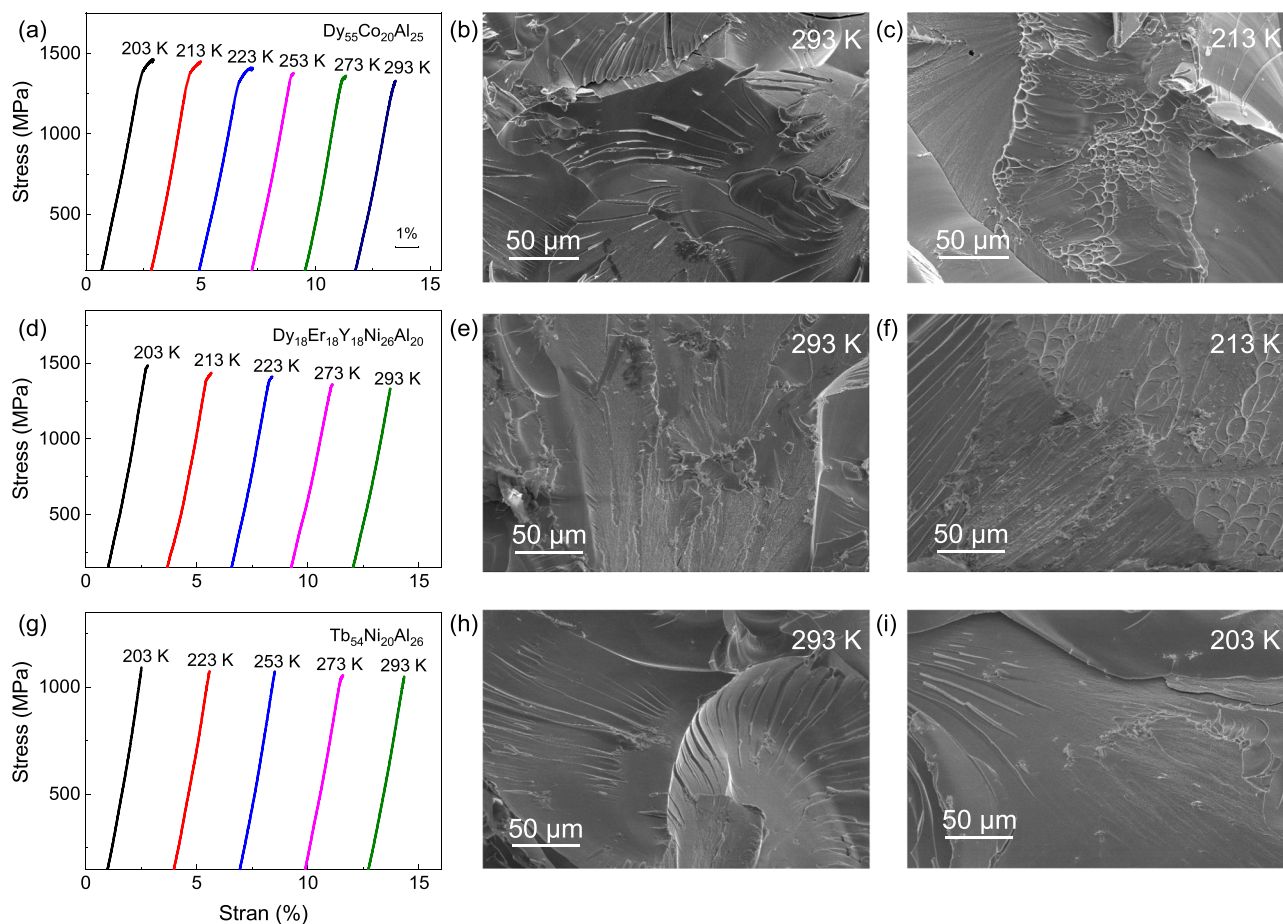


Fig. 2. The compressive stress versus strain curves at initial strain rate of $5 \times 10^{-4} s^{-1}$ with temperatures ranging from 203 to 293 K and SEM images of the fracture features for the (a)-(c) $Dy_{55}Co_{20}Al_{25}$, (d)-(f) $Dy_{18}Er_{18}Y_{18}Ni_{26}Al_{20}$ and (g)-(i) $Tb_{54}Ni_{20}Al_{26}$ BMGs.

S8 and $Pd_{40}Ni_{10}Cu_{30}P_{20}$ MG as shown in Fig. S10. These results provide additional evidence for the coexistence of γ relaxation and β' relaxation. Both of them belong to the fast process of secondary relaxation in MGs.

One of the features of a typical relaxation process is the frequency dependence. Fig. 1(c) shows the E'' spectra driven by different frequencies of the $Dy_{55}Co_{20}Al_{25}$ BMG. Two clear humps at low temperatures can be seen, and both of them shift to higher temperatures with increasing frequency. Voigt Amp. fitting was used to obtain the peak temperature as shown in Fig. 1(d). It is known that the frequency dependent peak temperature for secondary relaxation follows an Arrhenius relation, $f = f_0 \exp(-E_i/kT)$, where f_0 is the prefactor and k is the Boltzmann constant. E_i is the activation energy, and the subscript i denotes β , β' or γ relaxation. As shown in the inset of Fig. 1(c), the values of E_{β} and $E_{\beta'}$ are calculated to be 1.223 and 0.661 eV, that is to say, the value of $E_{\beta'}$ is approximately half of the E_{β} , which coincides with other heavy RE-based MGs [23,27]. However, the value of E_{γ} is fitted to be 0.446 eV, $\sim 2/3$ of $E_{\beta'}$, and smaller than the reported $E_{\beta'}$ (~ 0.6 eV) of most heavy RE-based MGs [23,27]. Therefore, it can be confirmed that different from β' relaxation, γ relaxation is an independent dynamic process with a lower activation energy.

Another feature of secondary relaxation is the correlation between the activation of relaxation and plastic deformation [19,27-29]. For example, unusual cryogenic plasticity of BMG has been reported and is attributed to the activation of β' relaxation [27]. As we elaborated above, the fast relaxation at ultralow temperature of some Zr-based BMG is reclassified into γ relaxation, which means that the activation of γ relaxation can also contribute to plastic events. To further substantiate this, a series of compression tests for the $Dy_{55}Co_{20}Al_{25}$ BMG from a temperature lower than the prominent γ relaxation region to room

temperature (RT) were performed. As shown in Fig. 2(a), the $Dy_{55}Co_{20}Al_{25}$ BMG sample exhibits brittle fracture with zero plasticity at RT, consistent with previous reports of the mechanical behaviors of heavy RE-based BMGs [30]. However, as the temperature decreases into the γ relaxation region, unusual plastic deformation of $\sim 0.6\%$ can be observed, especially for the curves at 213 and 223 K, which are near the peak temperature of γ relaxation (Fig. 1(d)). A similar brittle to ductile transition at the temperature range of γ relaxation is also found in a $Dy_{18}Er_{18}Y_{18}Ni_{26}Al_{20}$ high-entropy BMG showing coupled γ and β' relaxations at low temperatures (Fig. S5), although the plasticity is quite limited as shown in Fig. 2(d). In contrast, compression tests of the $Tb_{54}Ni_{20}Al_{26}$ BMG that only shows pronounced β' relaxation as displayed in Fig. S6 were also performed. One can see that absolutely brittle fracture is obtained at all testing temperatures, which further certifies that the activation of γ relaxation results in unusual cryogenic plasticity.

The fracture surface morphology provides important information on the dynamic fracture process and fracture mechanism of BMGs [31,32]. Generally, vein-like pattern which is also called the dimple structure, is the most commonly observed surface morphology on the fracture surface of some ductile Zr- and FeNi-based BMGs under compression tests [33-35]. As seen from Fig. 2(b), (e) and (h), all of the three BMG samples compressed at RT show typical brittle fracture morphology with no vein-like pattern, coinciding with their stress-strain curves. However, with compression near the peak temperature of γ relaxation, a number of vein-like patterns are observed on the fracture surface for the $Dy_{55}Co_{20}Al_{25}$ and $Dy_{18}Er_{18}Y_{18}Ni_{26}Al_{20}$ BMG samples as shown in Fig. 2(c) and (f). Among them, the vein-like patterns for the $Dy_{55}Co_{20}Al_{25}$ sample are more developed, thus leading to a larger plasticity at low temperature, and can be attributed to its more pronounced and

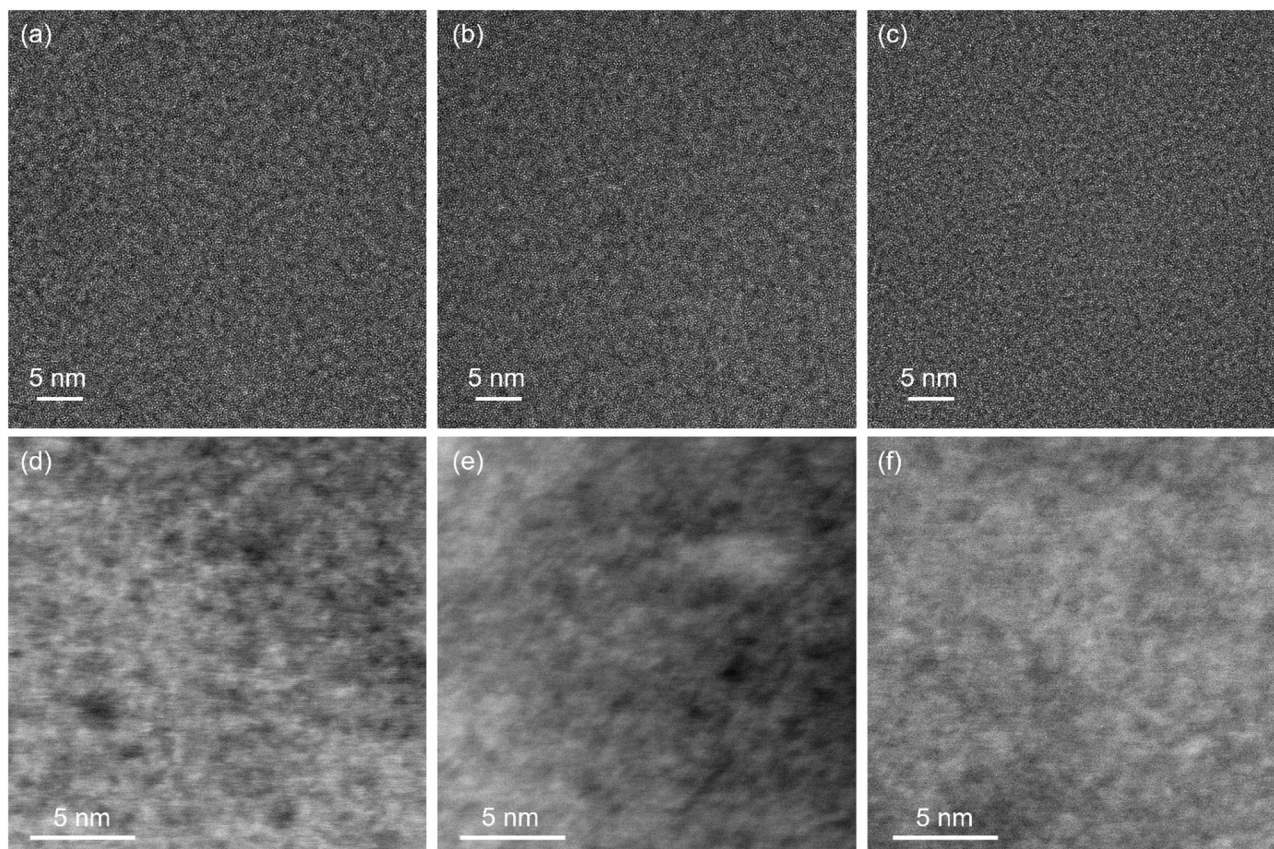


Fig. 3. HRTEM images of the (a) $\text{Dy}_{55}\text{Co}_{20}\text{Al}_{25}$, (b) $\text{Dy}_{18}\text{Er}_{18}\text{Y}_{18}\text{Ni}_{26}\text{Al}_{20}$ (c) $\text{Tb}_{54}\text{Ni}_{20}\text{Al}_{26}$ BMGs used for DMA measurements. (d-f) HAADF STEM images for the three samples.

decoupled γ relaxation hump. On the contrary, owing to the absence of γ relaxation, the $\text{Tb}_{54}\text{Ni}_{20}\text{Al}_{26}$ BMG sample still shows a completely brittle fracture morphology at cryogenic temperature. By all means, even for the $\text{Dy}_{55}\text{Co}_{20}\text{Al}_{25}$ and $\text{Dy}_{18}\text{Er}_{18}\text{Y}_{18}\text{Ni}_{26}\text{Al}_{20}$ samples, most areas of the fracture surface exhibit brittle features, resulting in very limited plastic deformation. Nevertheless, the fracture surface morphology provides robust evidence on linking cryogenic plasticity with γ relaxation.

Recently, a qualitative correlation between structural heterogeneity and β relaxation was provided [13,36]. Inspired by this, we try to unveil the underlying structural origin of γ relaxation from the viewpoint of structural heterogeneity. Fig. 3(a), (b) and (c) shows the HRTEM images of the $\text{Dy}_{55}\text{Co}_{20}\text{Al}_{25}$, $\text{Dy}_{18}\text{Er}_{18}\text{Y}_{18}\text{Ni}_{26}\text{Al}_{20}$ and $\text{Tb}_{54}\text{Ni}_{20}\text{Al}_{26}$ BMG samples, respectively. All samples display typical amorphous structures with maze-like features, and no distinguishable difference can be observed from the HRTEM images. Since high-angle annular dark-field scanning TEM (HAADF STEM) is sensitive to local chemistry and density, it is an effective method to characterize the nanoscale heterogeneity of MG. As expected, distinct contrast variation can be observed in HAADF STEM images for all BMG samples as shown in Fig. 3(d-f). It is seen that two obvious differences of the images can be observed. Firstly, the contrast for $\text{Dy}_{55}\text{Co}_{20}\text{Al}_{25}$ and $\text{Dy}_{18}\text{Er}_{18}\text{Y}_{18}\text{Ni}_{26}\text{Al}_{20}$ BMGs is more remarkable. Secondly, the apparent size of the dark region of $\text{Dy}_{55}\text{Co}_{20}\text{Al}_{25}$ and $\text{Dy}_{18}\text{Er}_{18}\text{Y}_{18}\text{Ni}_{26}\text{Al}_{20}$ BMG is smaller than that of the $\text{Tb}_{54}\text{Ni}_{20}\text{Al}_{26}$ BMG. According to previous studies, such contrast difference is associated with the nanoscale structural heterogeneity of MG [13,37], by ruling out the possible effect of elemental fluctuation on the image contrast as shown in Fig. S11. The bright regions in the HAADF STEM images possess relatively high density, while the dark regions contain lower density, i.e., dark regions are loosely packed regions (LPRs) [37]. Compared with the bright regions, the dark regions are more disordered because they possess order only in a rather short range together with

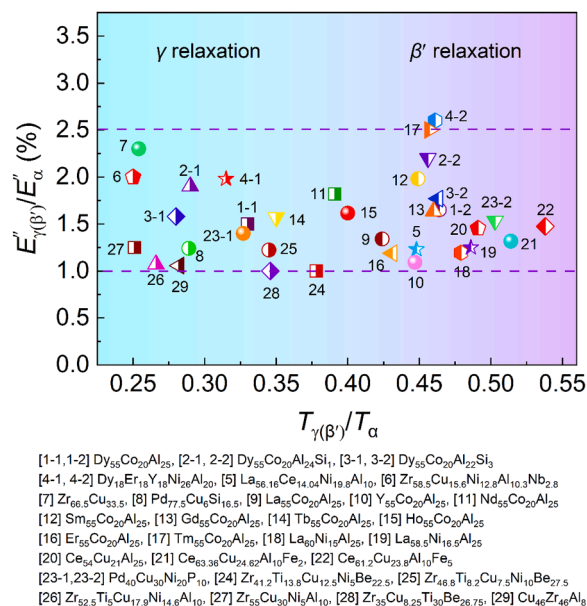


Fig. 4. Summary of fast secondary relaxation with the driven frequency of 1 Hz for various MGs plotted as $E''_{\gamma(\beta)}/E''_{\alpha}$ versus $T_{\gamma(\beta)}/T_{\alpha}$.

severe geometric distortion (“defects”) [37,38]. Therefore, the LPRs are supposed to play an essential role in the activation of low-temperature relaxations because of the high mobility of atoms.

The results in this study definitely indicate the existence of another fast relaxation in MGs, i.e., γ relaxation. To make a more comprehensive

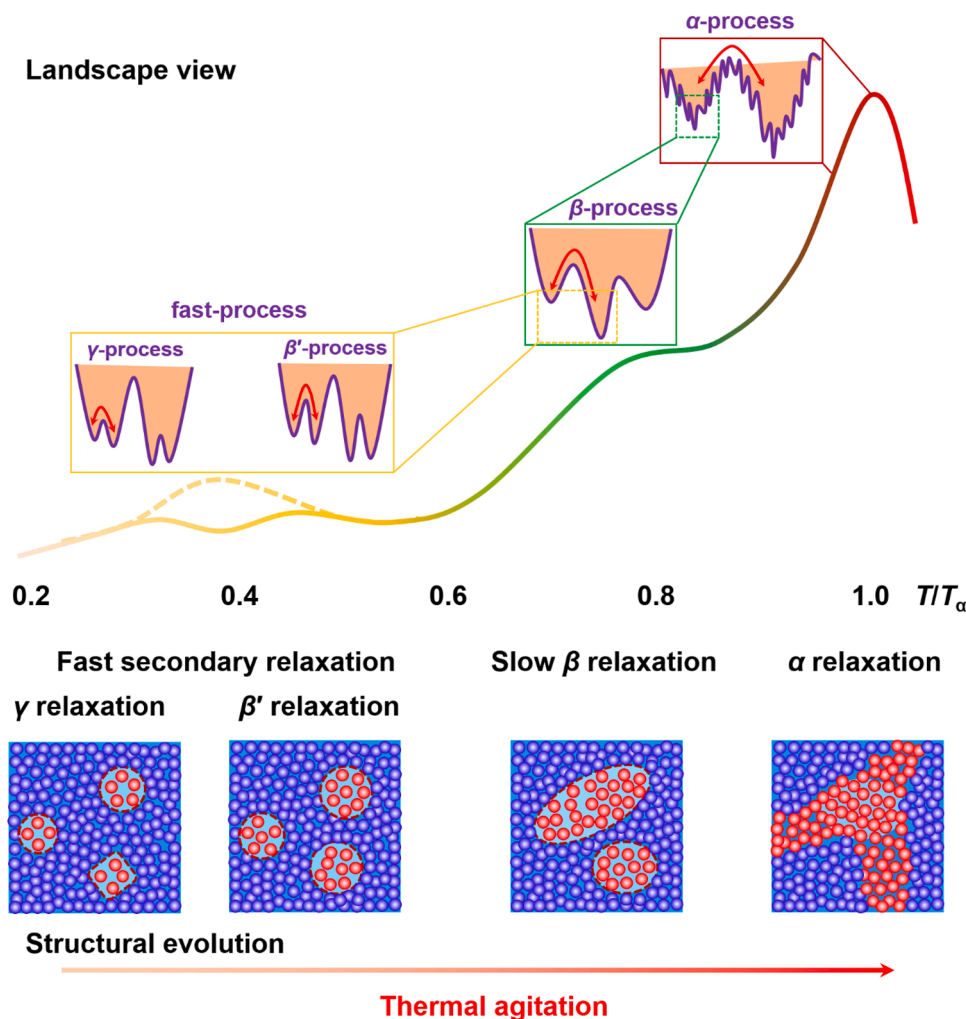


Fig. 5. Holistic picture of the relaxation modes in MGs based on the hierarchy of the PEL and corresponding structural evolution.

comparison between γ and β' relaxations, the relative values of loss modulus ($E''_{\gamma(\beta')}/E''_{\alpha}$) and peak temperature ($T_{\gamma(\beta')}/T_{\alpha}$) for the low-temperature relaxations obtained from multiple MGs were summarized in Fig. 4. At the first glance, there seems to be a cutoff point at $0.4 T_{\alpha}$, which is consistent with the observation of γ relaxation ($0.2\text{--}0.4 T_{\alpha}$) and β' relaxation ($0.4\text{--}0.6 T_{\alpha}$) in this study. Both the values of $E''_{\gamma(\beta')}/E''_{\alpha}$ for these two groups locates in $0.01\text{--}0.025 E''_{\alpha}$, and thus, there is no statistical distinction in relaxation strength for the two relaxation modes. Nevertheless, in the same MG system, β' relaxation exhibits a slightly higher strength than γ relaxation. At this point, based on the discovery of γ relaxation and the redefinition of β' relaxation, a more thorough DMS for MG can be concluded, as depicted in Fig. 5. At temperatures lower than 100 K ($< 0.1 T_g$) boson peak is activated firstly. With increasing temperature, localized γ relaxation picks up the baton giving rise to a detectable peak in DMS at temperatures near $0.3 T_g$ and evolves to another fast relaxation, β' relaxation at higher temperatures. As a precursor, the evolution of fast relaxation finally leads to the slow β relaxation mode which usually progresses at $0.7\text{--}0.9 T_g$. When the temperature further rises to T_g , α relaxation is activated and the overall disordered structure is broken, resulting in the final crystallization.

Next, another puzzling problem why only a single fast relaxation peak emerges on the DMS of most reported MGs will be discussed preliminarily by combining structural analyses and potential energy landscape (PEL) [39]. The two fast relaxations share similar structural motifs and energy states. The difference is that compared with β' relaxation, the average size of motif and the energy barrier for γ relaxation are slightly

smaller, as depicted in the schematic diagram of Fig. 5. As seen from the DMS of $\text{Dy}_{55}\text{Co}_{20}\text{Al}_{25}\text{Si}_1$ and $\text{Dy}_{55}\text{Co}_{20}\text{Al}_{25}\text{Si}_3$ BMGs in Figs. S3 and S4, the γ relaxation peak becomes unobvious compared with that of the $\text{Dy}_{55}\text{Co}_{20}\text{Al}_{25}$ BMG with the addition of Si element. In the previous study, we have demonstrated that increasing Si content induces the growth of local LPRs [40]. As a result, the structural motif suitable for γ relaxation decreases and the decoupling of γ relaxation and β' relaxation becomes harder. Whether the DMS of MG shows independent γ relaxation and β' relaxation depends on the scale and type of the local heterogeneous structure in MG. To be honest, the exact structural origin for fast secondary relaxation of MG is still elusive, which needs more advanced characterization and simulation in the future.

In summary, a novel fast γ relaxation is identified in several Dy-based MGs and this relaxation is universal in MGs by reclassifying the relaxation mode. A holistic relaxation spectrum of MG including boson peak, fast γ relaxation, fast β' relaxation, slow β relaxation and primary α relaxation is established. By fully activating γ relaxation, vein-like patterns develop in fracture surface, leading to unusual plasticity at cryogenic temperatures near the peak temperature of γ relaxation. The discovery of γ relaxation further enriches the variety of relaxation mode in MG and provides a novel viewpoint to unveil the origin of plasticity for MG.

Declaration of Competing Interest

The authors declare that they have no known competing financial

interests or personal relationships that could have appeared to influence the work reported in this paper.

Acknowledgements

This work was supported by the National Natural Science Foundation of China (Grant Nos. 51631003, 52101193, 51871140).

Supplementary materials

Supplementary material associated with this article can be found, in the online version, at [doi:10.1016/j.scriptamat.2022.115017](https://doi.org/10.1016/j.scriptamat.2022.115017).

References

- [1] N. Saba, P.M. Tahir, M. Jawaid, *Polymers* 6 (2014) 2247–2273.
- [2] M. Abdel-Baki, F. Ei-Diasty, *Curr. Opin. Solid State Mater. Sci.* 10 (2006) 217–229.
- [3] Y.H. Kim, J.S. Heo, T.H. Kim, S. Park, M.H. Yoon, J. Kim, M.S. Oh, G.R. Yi, Y. Y. Noh, S.K. Park, *Nature* 489 (2012) 128–U191.
- [4] H.X. Li, Z.C. Lu, S.L. Wang, Y. Wu, Z.P. Lu, *Prog. Mater. Sci.* 103 (2019) 235–318.
- [5] C.A. Angell, K.L. Ngai, G.B. McKenna, P.F. McMillan, S.W. Martin, *J. Appl. Phys.* 88 (2000) 3113–3157.
- [6] K.L. Ngai, *Relaxation and Diffusion in Complex Systems*, Springer, New York, 2011.
- [7] J.C. Qiao, Q. Wang, J.M. Pelletier, H. Kato, R. Casalini, D. Crespo, E. Pineda, Y. Yao, Y. Yang, *Prog. Mater. Sci.* 104 (2019) 250–329.
- [8] W.H. Wang, *Prog. Mater. Sci.* 106 (2019), 100561.
- [9] D.B. Miracle, *Nat. Mater.* 3 (2004) 697–702.
- [10] Y.Q. Cheng, E. Ma, *Prog. Mater. Sci.* 56 (2011) 379–473.
- [11] H.W. Sheng, W.K. Luo, F.M. Alamgir, J.M. Bai, E. Ma, *Nature* 439 (2006) 419–425.
- [12] Y.H. Liu, D. Wang, K. Nakajima, W. Zhang, A. Hirata, T. Nishi, A. Inoue, M. W. Chen, *Phys. Rev. Lett.* 106 (2011), 125504.
- [13] F. Zhu, H.K. Nguyen, S.X. Song, D.P.B. Aji, A. Hirata, H. Wang, K. Nakajima, M. W. Chen, *Nat. Commun.* 7 (2016), 11516.
- [14] Z. Wang, H.B. Yu, P. Wen, H.Y. Bai, W.H. Wang, *J. Phys-Condens. Mat.* 23 (2011), 142202.
- [15] H.B. Yu, W.H. Wang, K. Samwer, *Mater. Today* 16 (2013) 183–191.
- [16] H.B. Yu, W.H. Wang, H.Y. Bai, Y. Wu, M.W. Chen, *Phys. Rev. B* 81 (2010), 220201.
- [17] H.B. Yu, K. Samwer, Y. Wu, W.H. Wang, *Phys. Rev. Lett.* 109 (2012), 095508.
- [18] H.B. Yu, Z. Wang, W.H. Wang, H.Y. Bai, *J. Non-Cryst. Solids* 358 (2012) 869–871.
- [19] H.B. Yu, X. Shen, Z. Wang, L. Gu, W.H. Wang, H.Y. Bai, *Phys. Rev. Lett.* 108 (2012), 015504.
- [20] L.C. Zhang, Z. Jia, F. Lyu, S.X. Liang, J. Lu, *Prog. Mater. Sci.* 105 (2019), 100567.
- [21] L.L. Shao, L. Xue, Q. Luo, Q.Q. Wang, B.L. Shen, *Materialia* 7 (2019), 100419.
- [22] Q. Wang, S.T. Zhang, Y. Yang, Y.D. Dong, C.T. Liu, J. Lu, *Nat. Commun.* 6 (2015) 7876.
- [23] L.Z. Zhao, R.J. Xue, Z.G. Zhu, K.L. Ngai, W.H. Wang, H.Y. Bai, *J. Chem. Phys.* 144 (2016), 204507.
- [24] S. Kuechemann, R. Maass, *Scripta Mater* 137 (2017) 5–8.
- [25] D.E. Kline, *J. Polym. Sci.* 47 (1960) 237–249.
- [26] M. Schwabe, R. Rotzoll, S. Kuechemann, K. Nadimpalli, P. Vana, K. Samwer, *Macromol. Chem. Phys.* 211 (2010) 1673–1677.
- [27] Q. Wang, J.J. Liu, Y.F. Ye, T.T. Liu, S. Wang, C.T. Liu, J. Lu, Y. Yang, *Mater. Today* 20 (2017) 293–300.
- [28] Z.Y. Zhou, Q. Chen, Y. Sun, H.B. Yu, *Phys. Rev. B* 103 (2021), 094117.
- [29] J.C. Qiao, Y. Yao, J.M. Pelletier, L.M. Keer, *Int. J. Plasticity* 82 (2016) 62–75.
- [30] D. Chen, A. Takeuchi, A. Inoue, *J. Mater. Sci.* 42 (2007) 8662–8666.
- [31] B.A. Sun, W.H. Wang, *Prog. Mater. Sci.* 74 (2015) 211–307.
- [32] C.A. Schuh, T.C. Hufnagel, U. Ramamurty, *Acta Mater* 55 (2007) 4067–4109.
- [33] W.M. Yang, H.S. Liu, Y.C. Zhao, A. Inoue, K.M. Jiang, J.T. Huo, H.B. Ling, Q. Li, B. L. Shen, *Sci. Rep.* 4 (2014) 6233.
- [34] J. Zhou, Q.Q. Wang, Q.S. Zeng, K.B. Yin, A.D. Wang, J.H. Luan, L.T. Sun, B.L. Shen, *J. Mater. Sci. Technol.* 76 (2021) 20–32.
- [35] W.H. Zhou, F.H. Duan, Y.H. Meng, C.C. Zheng, H.M. Chen, A.G. Huang, Y.X. Wang, Y. Li, *Acta Mater* 220 (2021), 117345.
- [36] D.P. Wang, J.C. Qiao, C.T. Liu, *Mater. Res. Lett.* 7 (2019) 305–311.
- [37] F. Zhu, A. Hirata, P. Liu, S.X. Song, Y. Tian, J.H. Han, T. Fujita, M.W. Chen, *Phys. Rev. Lett.* 119 (2017), 215501.
- [38] A. Hirata, L.J. Kang, T. Fujita, B. Klumov, K. Matsue, M. Kotani, A.R. Yavari, M. W. Chen, *Science* 341 (2013) 376–379.
- [39] C.A. Angell, *Science* 267 (1995) 1924–1935.
- [40] L.L. Shao, Q.Q. Wang, L. Xue, M.Y. Zhu, A.D. Wang, J.H. Luan, K.B. Yin, Q. Luo, Q. S. Zeng, L.T. Sun, B.L. Shen, *J. Mater. Res. Technol.* 11 (2021) 378–391.